

Scaling in Plasticity-Induced Microstructure: Cell Boundary Misorientation Distributions.

James P. Sethna

Laboratory of Atomic and Solid State Physics (LASSP), Clark Hall, Cornell University, Ithaca, NY 14853-2501, USA

Eugene Demler

Physics Department, Lyman Labs, Harvard University, Cambridge, MA 02138

(February 7, 2020)

We study the scaling form for the cell boundary misorientation angle distribution of Hughes and co-workers. By formulating the problem in terms of random walks in rotation space, we are able to incorporate the new cell boundaries formed during cell re-nement with increasing deformation. The simplest form for the corresponding diffusion equation yields a good fit to the experimental scaling curve for the incidental boundaries, including the ϵ^{-2} scaling of the average angle and the linear slope at small angles. We consider effects of crystalline anisotropy and strain gradients, and show that they also allow scaling collapses but change the form of the scaling function (yielding scaling but not universality). Existing theories formulated in terms of uncorrelated random dislocation motion exhibit the experimental scaling of average angle only if cell re-nement is ignored.

from grain boundaries in that their misorientation angle across them is small (around a degree or less) and they form in a nonequilibrium process, typically at temperatures where diffusion is not relevant (so that the impurity segregation characteristic of many grain boundaries is not observed at cell boundaries). As deformation proceeds, the cell structure refines (the typical cell size L becomes smaller), and the average cell misorientation angle $\langle \theta \rangle_{av}$ grows. Hughes et al. observe that $L \langle \theta \rangle_{av}^{-1} \propto \epsilon^{-1/2}$, where ϵ is the magnitude of the net plastic strain. They find that data for several materials and different strain amplitudes all collapse onto an apparently universal scaling curve $\langle \theta \rangle_{av}$ when rescaled to the average angle:

$$\langle \theta \rangle_{av} = \epsilon^{1/2} \langle \theta \rangle_{av} \quad (1)$$

We will study the scaling of this probability distribution $P(\theta)$.

I. INTRODUCTION

A. Scaling and Universality in Plasticity?

Scaling and similarity are essential tools in the study of materials morphology. In engineering studies of plastic deformation, we have the principle of similitude [1]: a given material under a given deformation geometry will exhibit a characteristic morphology, with only the overall length scale changing with time. In physics, the study of second-order phase transitions has led us to expect scaling to be associated with universality [2]: the observed morphology near the critical point is expected to be independent of material. Under what circumstances can we expect not only similarity between the same material at different times, but also similarity between different materials, undergoing different deformations?

Hughes et al. [3,4] have observed experimentally that the shape of the probability distribution of misorientation angles $\langle \theta \rangle$ across incidental cell boundaries in stage III hardening is independent of material, suggesting universality. Briefly, there are several stages in the work hardening of a plastically deformed metal. Stage III is characterized by the segregation of the tangled dislocations into cell boundaries, separating nearly perfect crystalline called cells. These cell boundaries are distinct

The physics and engineering communities both use scaling in their studies of coarsening and spinodal decomposition. In binary fluid mixtures, there are clear regimes where phase separation yields scaling and universal correlation functions: the patterns formed by oil and water as they separate are not only the same after different waiting times, but are also the same as patterns formed by other immiscible fluid mixtures. There has been a widespread assumption in the physics community that this universality would extend also to binary alloy segregation and coarsening in Ising models. However, recent work [5] clearly shows that the crystalline anisotropy in the interface energy and interfacial growth velocities are relevant perturbations, which change the morphology but leave the scaling exponents unchanged. (This anisotropy went unrecognized in the Ising model because it was rather weak. It is much more striking when next-neighbor antiferromagnetic bonds are introduced. Indeed, in such models the anisotropy can produce a phase with sharp corners at low temperatures, associated with a change in the coarsening length from power-law to logarithmic in time [6].) Thus in the case of coarsening in crystals, there is scaling (similitude) but not universality (independence of material). A key question for us is whether Hughes' measurements really go beyond similitude and involve true universality.

We develop a phenomenological model here for the evolution of $\langle \theta \rangle$, using the orientations of the cells as our basic variables. In section III we will treat the evolution of the misorientation at a given cell boundary as a simple random walk in rotation angle space, and incorporate the cell re-nement by adding new cell boundaries (dividing existing cells) which start at zero misorientation angle. We observe the experimental scaling $\langle \theta \rangle_{av} \propto L^{-1/2}$ and derive a prediction for the scaling form $\langle \theta \rangle_{scaling}(\cdot)$. In section IV we will incorporate an imposed strain gradient in the geometry of the experiment by adding a drift term to the random walk in angle space. We find the experimental scaling, with a different distribution function $\rho_{drift}(\theta; v_0)$ depending on the relative size v_0 of the strain gradient. These strain gradients could arise from natural inhomogeneities in a polycrystalline sample: they could also be applied directly using experiments on small samples. In section V we generalize our model to allow for crystalline anisotropy in the random walk diffusion constant, to make contact with earlier theories of the misorientation angle distribution [7-10]. The earlier theories used dislocations as their basic variables, and did not incorporate cell re-nement. We will show how to interpret their work in our framework, but will demonstrate that incorporating cell re-nement changes the predictions of the dislocation theories from the observed $L^{-1/2}$ scaling to $\langle \theta \rangle_{av} \propto L^{-3/4}$. In the end, we find that (as for correlation functions in coarsening in crystals) the scaling curve for $\langle \theta \rangle$ should depend upon material and details of the experiment, but that the dependence is not strong.

To put our work in perspective, a brief list of problems in plasticity that we do not address would seem appropriate.

(1) We do not address the organization of dislocations into cell walls in stage III hardening. Does energy minimization or dynamical pattern formation govern the formation of these structures? By organizing into cell walls the dislocations certainly lower their energy [1,11]. On the other hand, the mobility of a dislocation certainly is much higher when the dislocation density is low, so the dynamics will be unstable to clumping.

(2) We do not explain the two types of cell boundaries. Hughes et al. found that the good scaling collapse seen in figure 2 was obtained not for the full distribution of cell boundary misorientations, but only after the boundaries were restricted to what were termed incidental dislocation boundaries (which we refer to as incidental cell boundaries since our approach ignores the dislocations). They draw a distinction between these boundaries and what they term geometrically necessary boundaries. (Unlike geometrically necessary dislocations, these boundaries appear not to be connected with strain gradients.) The experimental separation between the two

types of cell boundaries was primarily morphological (the geometrically necessary boundaries are long and nearly planar, and enclose several cells divided in the cross direction by incidental boundaries). These geometrically necessary boundaries introduce a second length scale, which in principle will spoil scaling (one expects a qualitative change in behavior when the spacing between geometrically necessary boundaries crosses that of the incidental cell boundaries). The spacing L_{GNB} between the geometrically necessary boundaries is typically larger than that L between the incidental boundaries, but their typical spacing shrinks faster ($L_{GNB} \propto L^{-2/3}$). Hence at late times they must become important, but conversely at early stages in stage III we may ignore them [4].

(3) We do not address the spatial arrangements of the incidental cell boundaries. In particular, we incorporate the experimentally observed re-nement of the cells $L \propto t^{-1/2}$ by hand. (In section III, we do discuss the length scaling implied by the naive mechanism for cell re-nement, but we show that it gives the wrong power law, $L \propto t^{-1/3}$.) A complete theory should also discuss the observed scaling distribution of cell boundary separations [4]. Since one of our conclusions is that these scaling distributions should depend upon the material and the geometry of the experiment, a complete theory may not be simple.

II. MATHEMATICS OF CELL EVOLUTION

To start, we need a few elementary mathematical facts about the geometry of a cross a cell boundary. Imagine a cell boundary as in figure (1). We will study the distribution of misorientation angles in terms of the misorientation matrix $R_L R_R^{-1}$, which is the rotation needed to take the right-hand cell to the orientation on the left-hand side. We can write this rotation as $\exp(n \cdot J)$, where the matrix $J_i = \epsilon_{ijk}$ (with ϵ_{ijk} the totally antisymmetric tensor) generates an infinitesimal rotation about the i^{th} axis. The misorientation across all of our cell boundaries is small, so we can expand our matrix in n . (Large angle corrections are discussed in [9] and [12].) To the order we need it $\mathcal{O}(n^3)$ on the diagonal, $\mathcal{O}(n)$ off-diagonal,

$$R_L R_R^{-1} = \begin{pmatrix} \exp(n \cdot J) & & & \\ & 1 & & \\ & & 1 & \\ & & & 1 \end{pmatrix} + \begin{pmatrix} 0 & n_3 & n_2 & 0 \\ n_3 & 0 & n_1 & 0 \\ n_2 & n_1 & 0 & 0 \\ 0 & 0 & 0 & 0 \end{pmatrix} + \begin{pmatrix} \frac{n_2^2 + n_3^2}{2} & n_3 n_2 & n_2 n_1 & 0 \\ n_3 n_2 & \frac{n_1^2 + n_3^2}{2} & n_1 n_2 & 0 \\ n_2 n_1 & n_1 n_2 & \frac{n_1^2 + n_2^2}{2} & 0 \\ 0 & 0 & 0 & 0 \end{pmatrix} \quad (2)$$

and the misorientation angle is

$$\text{Tr}(R_L R_R^{-1}) = 1 + 2 \cos \theta \approx 3 - \frac{2}{3} \theta^2 = 3 - \frac{2}{3} n_j n_j \quad (3)$$

Define $\Omega(n)$ to be the area of cell boundary with misorientation matrix $\exp(n \cdot J)$. If this distribution is spheri-

cally symmetric, equation (3) implies that the probability distribution for the misorientation angle

$$P(\theta) = P(\theta) = 4 \pi^2 \sin^2(\theta) = d^3 n(\theta) \quad (4)$$

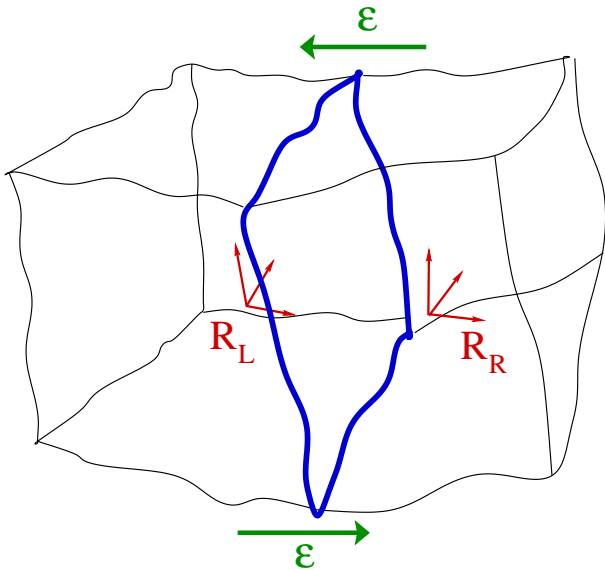


FIG. 1. Geometry of a Cell Boundary.

We note that there are three different probability distributions that might be of interest to measure, depending on how one weights boundaries in terms of their characteristic size L . We will work with the probability distribution for the misorientations per unit area of cell boundary, weighting them by L^2 . Another natural measure is to weight the cell boundaries equally, independent of their relative areas. The experimental measurements [3] weight each cell boundary observed in a given two-dimensional cross-section equally: this of course gives larger weight to those boundaries with larger spatial extent perpendicular to the experimental cross-section plane, effectively weighting each boundary by L . In our analysis, the dependence of L on time (or net deformation) will be important, but we will ignore the distribution of domain sizes at a given time: in this approximation these three distributions are all the same.

III. THE ROTATIONAL DIFFUSION MODEL

We begin with a simple model of the time evolution of the distribution of misorientation matrices across incidental boundaries $\rho(n)$: a diffusion equation with a source term:

$$\frac{\partial \rho(n)}{\partial t} = D \nabla^2 \rho + C \rho^{1-2} \quad (5)$$

where the gradients on the right are with respect to n . Here C is a scalar which represents the magnitude of the

net plastic deformation. Presuming the experiment is performed quasistatically with a shear rate constant in time, here can be thought of as the time elapsed.

The first term in equation (5) represents a diffusion, or random walk, in rotation space. (Composing small incremental rotations is equivalent to adding the corresponding vectors n , since $\exp(n_1 J) \exp(n_2 J) = \exp((n_1 + n_2) J) + O(\dot{n})$.) We imagine that the two cells on either side of the boundary are exposed to slightly different shears and torques, and that these differences change randomly and relatively rapidly as the shear increases. Since diffusion equations have root-mean-square displacements which grow as the square root of time, this term is obviously suggested by the experimental observation that $\rho \sim t^{-1/2}$.

The second term in equation (5) represents the creation of new cell boundaries which divide the old ones. There are various proposed mechanisms for adding to the cell boundary area to allow the cell sizes to shrink. Abstractly, one could imagine new cells nucleating at intersections of old cells, or imagine the cell boundaries crinkling. Both of these mechanisms, however, involve the motion of existing cell boundaries, which is difficult because of the pinning by sessile dislocation junctions [13]. The mechanism we propose is the formation of new cell boundaries dividing old cells. The old cell boundaries in our picture do not move. The new cell boundary, where it terminates at the old cell boundaries, will divide them into unequal halves which will thereafter evolve separately under the diffusion equation. Because we choose to weight our misorientation angle density according to the boundary area, this division does not change the cell boundary density $\rho(n)$ except at $n = 0$.

(As an illustration of how power law refinement could arise, consider a simple but apparently incorrect model where dislocation collisions create new cell boundaries. When they collide, they form a sessile junction in the interior of a cell; further dislocations passing through the cell form a net as they catch on the two original ones [14]. Suppose during a time T our material goes through a strain increment ϵ . The number of dislocations passing through a cell of size L goes as $N = L/\lambda = b/\lambda$, where b is the Burgers vector or the lattice constant. The time each dislocation spends passing through the cell scales as $t = L/v$ where the dislocation velocity v is often rather large. The fraction of time a cell is occupied by one of the dislocations, then, will scale as $N t$. Presuming more than one slip system is active, the chance that a given dislocation will collide with one on a different slip system is given by the fraction of time the cell is occupied by dislocations of the other slip system, roughly proportional to $N t = T$. The probability of a collision for N dislocations (and hence a cell division) is then $N^2 t = T$. Such a collision reduces the cell size by a factor of two, and hence changes $\log L$ by a factor of $\log 2$, so

$$\begin{aligned}
\log L &= (\log 2)N^2 \quad t = T \\
(L = b)^2 \quad (L = v) \quad (1 = T) \\
(L^3 = bv) \quad (= T) \\
d \log L = d &= (1=L)dL = d \\
(L^3 = bv)d &= dT \\
L() &= L^{1=3} : \quad (6)
\end{aligned}$$

Hence this mechanism predicts the wrong power law ($\alpha=3$ rather than the experimental $\alpha=2$); it also predicts a dependence on the strain rate $d = dT$ which is also not observed. Perhaps, as suggested in reference [13], the dislocations moving through the cell may be pinned by obstacles; perhaps new cell walls are induced not through dislocation collisions but through torsional stresses introduced from neighboring cells.)

The new boundary area shows up in our distribution at zero misorientation angle (θ). To derive the amount of new boundary area which is created per unit strain, we note that the cell re-orientation is measured to be $L^{-1/2}$. The total boundary area will scale as the number of boundaries $1=L^3$ times the area per boundary L^2 , hence as $L^{-1/2}$. The new boundary area needed per unit time thus scales as $L^{-1/2}$, giving the prefactor for the ρ -function in equation (5).

If we start with no cell boundaries at $t = 0$, then the solution to equation (5) is

$$\begin{aligned}
\rho(\theta) &= \int_0^{\theta} du C u^{-1/2} \\
&= C \exp(-\theta^2/2D) = \frac{C}{\sqrt{2D}} \exp(-\theta^2/2D) \quad (7) \\
&= C \exp(-\theta^2/2D) = (2D)^{-1/2} \exp(-\theta^2/2D)
\end{aligned}$$

(The cell boundaries which are formed at deformation u have spread out into a Gaussian of variance $D(u)$) The total boundary area is $2C \int_0^{\theta} u^{-1/2} du$, as desired. This leads to a prediction for the probability distribution of misorientation angles that yields the scaling collapse (1)

$$\begin{aligned}
\rho(\theta) &= \frac{1}{\sqrt{2D}} \exp(-\theta^2/2D) \\
&= \frac{1}{\sqrt{2D}} \exp(-\theta^2/2D) \quad (8)
\end{aligned}$$

where

$$\frac{1}{\sqrt{2D}} = \frac{1}{\sqrt{2D}} \quad (9)$$

and

$$\text{scaling}(\theta) = (\theta^2/2D) \exp(-\theta^2/2D) \quad (10)$$

As we will discuss in section V, this happens to be the distribution as derived by Pantelon [7,8] in a model with out cell re-orientation.

One can see from figure 2 that the predicted form is quite a good description of the experimental data. This particular functional form is derived using $L^{-1/2}$, but the particular exponent is not crucial to the analysis: the solution for $L^{-\alpha}$ has this general form (with linear slope at $\theta = 0$ and $\rho(\theta) \sim \exp(-\theta^2/2D)$) for a wide range of powers α .

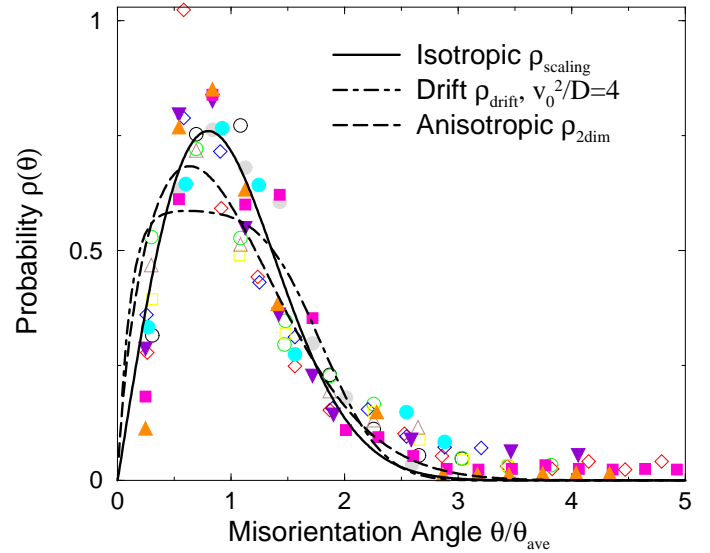


FIG. 2. Experiment vs. Theories. Experimental data digitized from Hughes et al. [3]. The solid curve is ρ_{scaling} , the scaling function of equation (10). The dot-dashed curve is ρ_{drift} , the scaling function for an experiment whose geometry imposes a strain gradient of relative strength $v_0^2/D = 4$ (see text). The dashed curve is $\rho_{\text{anisotropic}}$, the solution of equation (20) with a length-independent diffusion constant with one zero eigenvalue, representing a highly anisotropic rotational diffusion. While these theoretical curves differ, they all exhibit the same scaling exponent and have reasonably similar shapes. We predict that the scaling function will depend on material and strain geometry, which perhaps is consistent with the experimental data shown.

IV. THE DRIFT DIFFUSION MODEL

In equation (5), we've incorporated a rotational diffusion but have ignored the likely possibility that the cell boundary misorientation may have a monotonic drift term. Each cell, for example, will rotate due to the external shear unless the crystalline axes are aligned with the external shear. (This is the mechanism for texture evolution under strain.) These effects will be small, because the two cells on either side of the boundary are nearly of the same orientation and undergo nearly the same stress.

More important will be cases where the differences in torques across the cell boundary are due to long-range, ordered effects of the external loading: for example when strain gradients are imposed [15]. Bending a thin plate or wire of thickness d , for example, introduces a strain gradient per unit strain

$$d(\epsilon) = d^{-1/2} = d \quad (11)$$

This strain gradient will introduce a net rotational velocity of one cell with respect to another of

$$v = d \dot{\theta}$$

$$= L d(r) = d \quad (12)$$

where L is the current cell size. This average rotational velocity will be split in some way among the geometrically necessary cell boundaries and the incidental boundaries; for the purposes of this analysis we will ignore (as in the rest of the paper) the geometrically necessary boundaries. In combination with experimental scaling

$$L_{av} = A v_0^{p-1} \quad (13)$$

this gives

$$v = v_0 = v_0^{p-1} \quad (14)$$

where

$$v_0 = A d(r) = d \quad (15)$$

Strain gradients could also arise due to polycrystalline and polyphase inhomogeneities in the material.

Adding this drift term to the diffusion equation, we find

$$\frac{\partial \langle n \rangle}{\partial t} = (v_0^{p-1}) r + D r^2 + C^{-1/2} \langle n \rangle \quad (16)$$

We will see that this new term leads to a scaling collapse with v_0^{p-1} , equation (1), but with a function that depends on the ratio v_0^2/D :

$$\langle n \rangle ; v_0 = v_0^{1-p} \text{drift} (v_0^2/D) \quad (17)$$

A simple calculation gives for the solution of (16)

$$\langle n \rangle = C \int_0^Z \frac{du}{u} \frac{1}{(2D)^{3/2} (u)^{3/2}} \exp \left[-\frac{(n - 2v_0^{1-p} u^{1/2})^2}{2D (u)} \right] g \quad (18)$$

The probability distribution for the angle n (i.e., the absolute value of n) can be obtained by integrating over the directions of n (solid angle Ω)

$$\begin{aligned} \text{drift} (n ; v_0) &= \text{drift} (n ; v_0) = \frac{n^2 R}{d^3 n} \langle n \rangle \\ &= \frac{r}{D} \frac{n^2 D}{v^2} \int_0^{1/2} \frac{dx}{4x^{1/2} (1-x)^{3/2}} \\ &\quad \left[1 + \frac{p-1}{x} \sinh^{-2} \frac{n^2 v^2}{D} \right]^{-1} \\ &\quad \exp \left[-\frac{n^2}{D} \frac{1}{2(1-x)} - \frac{v_0^2}{D} \frac{1}{1-x} \frac{p-1}{x} \right] \quad (19) \end{aligned}$$

Equation (19) is the inverse of our old average misorientation angle from equation (9) times a function of n^2/D and v_0^2/D . Therefore, the new average misorientation angle scales as some function of v_0^2/D times $\frac{p-1}{D}$, and our density has the scaling form (17).

In Figure 2 we show the form of our scaling function $\text{drift} (v_0^2/D) \text{ for } v_0^2/D = 4$. For $v_0 = 0$ we of course get the original scaling; as $v_0 \rightarrow \infty$ the distribution becomes rectangular: $(2-x)=2$.

How thin a wire do we need to bend to see an observable change in our predicted distribution? Reference [4] observes that $L_{av} = 80b$ (where b is the Burgers vector), and gives data for v_0 ; using these values and equations (9), (13), (11), and (15) we estimate $D = 8 \cdot 10^{-4}$, $A = 2250b$, and $v_0^2/D = (A^2/D)4 = (160;000b)^2$. To make $v_0^2/D = 4$ for this experimental material, we'd need to bend a wire or sheet of thickness $80;000b$, somewhat over 10^{-3} cm.

The reason why the drift term added in (16) doesn't spoil the scaling form comes indirectly from the experimentally observed cell size scaling $L_{av} \propto v_0^{1/2}$, which implied that $v \propto v_0^{1/2}$. This velocity leads to angular trajectories $\propto v_0^{1/2}$ with the same scaling as for the diffusive motion. Hence both terms are of the same order, and the scaling collapse (17) still works but with an altered scaling function.

V. THE ANISOTROPIC DIFFUSION MODEL AND PANTELEON'S ANALYSIS

The distribution for the misorientation angle for the simple rotational diffusion model, $\text{scaling} (x)$, happens to have the same form as one derived by Panteleon [7,8] without considering cell re-nement, and by assuming that the noise in the cell orientations was due to random, uncorrelated fluctuations in the dislocation flux. It behooves us, therefore, to discuss how Panteleon's work can be interpreted in our context.

Panteleon's theory, also suggested by Nabarro [10] and Argon and Haasen [14], is that the stochastic noise in the flux of dislocation from either side of the cell boundary leads to randomness in the evolution of the cell boundary angles. Each dislocation passing through a cell, say, may shift the top plane of atoms by a distance b with respect to the bottom plane, where b is the Burgers vector of the dislocation (roughly the lattice constant). The crystalline axes within a cell of characteristic height L will rotate due to one dislocation an amount proportional to b/L . Under a strain increment ϵ , a cell of characteristic height L must have $N = L/b \epsilon$ dislocations impinging on the side cell boundary. A roughly equal and opposite average flux will impinge on the cell boundary from the cell on the other side. If the dislocations move independently (which we will argue does not occur), then one expects that there will be a net residue after the strain increment of roughly $N = L/b \epsilon$. Hence the predicted drift in angle after a strain increment of ϵ is $\epsilon = \frac{p-1}{N} \frac{1}{b} = \frac{p-1}{b} \epsilon = \frac{p-1}{L} \epsilon$. The diffusion constant is given by $D(L) \propto (b/L)^2 = \frac{b^2}{L^2}$. Because a single dislocation produces a larger net

rotation for smaller cell, the stepsize in the random walk in rotation space becomes larger as our cells get smaller.

Pantoleon and Hansen [9] consider three cases, where one, two, and three slip systems are activated. The geometry of a given cell (the direction and strength of the applied shear with respect to the crystalline axes) will determine what types of dislocations are allowed to pass through the cell. If only one slip system is active, the rotation of the cell will be confined to a single axis. In our formulation, the dislocation constant in rotation space will be anisotropic: in this case it will be a rank one tensor (a 3x3 matrix with only one non-zero eigenvalue). Two slip systems will give a rank 2 tensor, with one zero eigenvalue. Three slip systems will allow the cell to diffuse in any direction, but even so the dislocation constant D will in general be anisotropic.

To make contact with Pantoleon, we consider a more general evolution law for the misorientation:

$$\frac{\partial \langle n \rangle}{\partial t} = D_{ij}(L) r_i r_j + C^{-1} \langle n \rangle \quad (20)$$

Here we have allowed for an anisotropic, cell-size-dependent dislocation constant by introducing the symmetric tensor $D_{ij}(L)$ depending on the current cell size L . The symmetric dislocation tensor D_{ij} will vary with the geometry of the particular cell boundary: it can depend both on the relative orientation of the crystal and the strain tensor with respect to the plane of the cell boundary. We have also introduced new boundaries to be compatible with the more general scaling L^{-a} discussed above. (As noted in section IV, changing this power in the presence of strain gradients would spoil the scaling collapse.)

Pantoleon [7,9] in most of his analysis ignores cell re-orientation. If we make D_{ij} independent of L and set $C = 0$ in equation (20), we get an anisotropic diffusion equation whose solution (assuming a narrow initial distribution of misorientations) is an anisotropic Gaussian with variances given by the inverse eigenvalues of D , with the experimentally observed scaling $\langle \theta \rangle_{av}^{-1} = 2$. If we assume D has one non-zero eigenvalue, we get the Gaussian distribution derived by Pantoleon and Hansen for one active slip system. If we assume D has two equal, non-zero eigenvalues, we get the Rayleigh distribution that they found for two perpendicular systems of edge dislocations (which, coincidentally, is the same distribution that we found above (10) with an isotropic D and a source term). If we assume D is isotropic, we get the Maxwell distribution they found for three perpendicular systems of dislocations.

What happens to the solution of equation (20) when we incorporate cell re-orientation? Pantoleon [8] notices that non-constant cell size must change the scaling of average angle with strain. By setting $D(L) = D_0 L^{-a}$ and changing variables to $\theta = \theta' L^{1+a}$ in equation (20), we can map it into a problem quite similar to equation (5) except that the

source term is of magnitude proportional to $L^{-(1+a)}$. The solution to this equation has a shape quite similar to that shown in figure (2), but with an average angle $\langle \theta \rangle_{av} = \frac{1}{(1+a)^2}$. This yields a $3/4$ power of the strain using the length scaling $a = 1/2$ of reference [4], incompatible with the scaling observed for the incidental cell boundaries. Pantoleon is aware of this problem [8]: in his analysis he uses $a = 0.42$ and gets a $(1+a)^{-2} = 0.71$ power of strain, in disagreement with the experiment.

Although Pantoleon's microscopic calculations were based on a faulty premise of uncorrelated dislocation motion, his analysis did point out that the individual cell boundaries have rather low symmetries. The dislocation tensor in equation (20) describes the evolution of that subset of cell boundaries with a particular cell boundary orientation and (average) crystal lattice orientation with respect to the external shear. There is no reason that for a low-symmetry geometry that the dislocation constant will be isotropic, geometry dependent, or material dependent: the general evolution law is (20) with D_{ij} independent of L . One must solve for the distribution at fixed geometry and then average over geometries to predict the experimental distribution (as also discussed in section 5.2 of reference [9]). If we assume a strongly anisotropic rotational dislocation tensor with one zero eigenvalue and the other two equal (corresponding roughly to Pantoleon's analysis with two active slip systems) we can solve equation (20) to find a scaling collapse (1) with scaling function

$$2d_{im}(\mathbf{x}) = \left(\sqrt{3}x=64 \right) \exp\left(-\sqrt{3}x^2=128 \right) K_0\left(\sqrt{3}x^2=128 \right) \quad (21)$$

where K_0 is the modified Bessel function of the second kind. This scaling function is shown in figure (2).

V I. CELL ROTATIONS V S. D ISLOCATIONS : W H I C H V A R I A B L E S T O U S E ?

What is wrong with the dislocation shot noise mechanism? The problem is not that the magnitude of the noise is small: estimates suggest [10,8] that it would be roughly the right magnitude to explain the experiments. But the dislocation mechanism inescapably leads to the wrong scaling of angle with strain.

We attribute the problem to the assumption that the dislocations slip independently. The interaction energy between dislocations is large, and diverges logarithmically with distance, reflecting the infinite stiffness of a crystal to gradients in the axes of rotation. In stage I and stage II hardening, one might plausibly argue that the dislocations are sufficiently far apart that their interaction forces do not dominate. But in stage III, the fact that the dislocations organize into boundaries (avoiding rotational distortions within the cells) is a clear signal

- [12] D. P. Miska and P. R. Dawson, *Acta Materialia* 47, 1355 (1999).
 N. R. Barton and P. R. Dawson, "On the spatial arrangement of lattice orientations in hot rolled multi-phase titanium", to be published.
- [13] F. Prinz and A. S. Argon, *Physica status solidi* 57, 741, (1980). They discuss not collisions between dislocations on different slip systems, but mutual trapping of dislocations with opposite Burgers vector on one slip system: our analysis still applies. One should note that Argon now believes that cell boundaries may move during plastic deformation through avalanches of failures of these sessile dislocation junctions.
- [14] A. S. Argon and P. Haasen, *Acta Metall. Mater.* 41, 3289, (1993) equation 21.
- [15] N. A. Fleck, G. M. Muller, M. F. Ashby, J. W. Hutchinson, *Acta Mater.* 42, 475-487 (1994).